JOURNAL OF CATALYSIS 147, 250–263 (1994)

Alkyl Chain Propagation by Methylene Insertion on Cu(100)

Jong-Liang Lin,[1] Chao-Ming Chiang,[2] Cynthia J. Jenks,[3] Michael X. Yang, Tim H. Wentzlaff, and Brian E. Bent[4]

Department of Chemistry, Columbia University, New York, New York 10027

Received September 8, 1993; revised November 15, 1993

One of the mechanisms proposed for formation of carbon–carbon bonds in the Fischer–Tropsch synthesis, the so-called carbide/methylene mechanism, involves the propagation of alkyl chains on the catalyst surface by methylene insertion. The studies reported here provide evidence for this reaction on single crystal copper surfaces under ultra-high vacuum conditions. Alkyl iodides are used as molecular precursors to generate adsorbed methylene and alkyl groups on a Cu(100) surface. High-resolution electron energy loss spectroscopy and work function change measurements show that C–I bond dissociation occurs below 200 K in iodoalkanes to form alkyl groups on the surface. Indirect evidence supports the formation of adsorbed methylene groups via CH_2I_2 dissociation. Temperature-programmed reaction studies of the $CH_2 + CD_3$ reaction show that sequential CH_2 insertion followed by β-hydride elimination produces ethylene-d_2 and propylene-d_3. Similarly, reaction of CH_2 with C_2D_5 produces propylene-d_4. All of these reactions are extremely facile, occurring at 230–250 K with activation energies of 12–20 kcal/mol. Similar studies on Cu(110) show that the methylene insertion reaction is structure sensitive, being approximately two orders of magnitude faster on Cu(100) than on Cu(110). The source of this difference appears to be slow diffusion of methylene across the corrugated Cu(110) surface. © 1994 Academic Press, Inc.

1. INTRODUCTION

A key feature of the Fischer–Tropsch reduction of carbon monoxide by hydrogen over transition metal catalysts is the formation of carbon–carbon bonds and the production of higher hydrocarbons. Despite the more than 65 years since the discovery of this reaction (1), the pathways by which carbon–carbon bonds are formed remain controversial. Numerous mechanisms have been proposed, and it is likely that more than one may play a role (2). The challenge is to obtain experimental evidence for each of the mechanisms proposed and to understand the factors that favor one reaction pathway over another.

One of the contributions that can be made by studies of single crystal surfaces under ultra-high vacuum conditions is to establish chemical precedence for proposed surface reaction pathways in catalytic processes. For example, the formation, identification, and spectroscopic characterization of proposed reaction intermediates on well-defined surfaces provide insight into the basic features of chemical structure and bonding at surfaces. Less well demonstrated, but potentially even more important, is the possibility that if the appropriate reaction intermediates can be generated and isolated on the surface in high concentration, then reactions typically observed only under catalytic reaction conditions might also occur in vacuum where electron spectroscopies, isotope labeling, and mass spectrometry can be applied to determine the surface reaction mechanisms (3). While the reaction conditions in such studies are undeniably quite different from those in a catalytic process, the results can provide chemical insight into proposed catalytic reaction pathways.

In this paper we report such a study of the proposed carbide/methylene mechanism of carbon–carbon bond formation in the Fischer–Tropsch reaction. This mechanism is shown schematically in Fig. 1. A large number of studies (4) have provided convincing evidence for various aspects of this pathway under catalytic reaction conditions including the presence of carbidic carbon (5), the hydrogenation of carbidic carbon (6), the formation of alkyl groups (7), and the role of methylene (CH_2) as the active chain growth species (8). There have also been a number of reports on the bonding and reactions of methylene (9) and alkyl (10) groups formed on single crystal metal surfaces under vacuum conditions by the thermal, photochemical, or electron-induced dissociation of molecular precursors such as alkyl halides and azoalkanes (9, 10). Few studies, however, have addressed reactions been coadsorbed hydrocarbon fragments. Recently, we have shown, as summarized in Scheme 1, that when CH_2I_2 and CD_3I are thermally dissociated on a Cu(110) surface

[1] Present address: Department of Chemistry, University of Pittsburgh, Pittsburgh, PA 15260.

[2] Present address: AT&T Bell Laboratories, Murray Hill, NJ 07974.

[3] Present address: Department of Chemistry, Iowa State University, Ames, IA 50011.

[4] To whom correspondence should be addressed.

0021-9517/94 $6.00

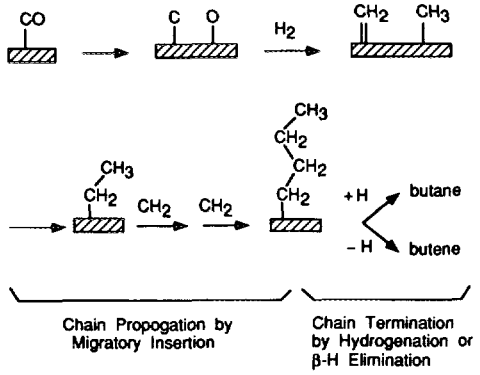

FIG. 1. Schematic illustration of the carbide/methylene surface reaction mechanism for formation of higher hydrocarbons during the Fischer–Tropsch reduction of carbon monoxide with hydrogen.

to form adsorbed CH_2 and CD_3, migratory insertion occurs at ~315 K to form CH_2CD_3 which undergoes β-hydride elimination to evolve ethylene-d_2 (11).

This reaction is exactly that proposed for forming C–C bonds in the carbide/methylene mechanism of the Fischer–Tropsch reaction. On Cu(110), however, longer alkyl chains are not formed because chain termination by β-hydride elimination is fast compared with the rate of alkyl chain propagation by methylene insertion. Here, we report results which show that, on the smoother Cu(100) surface, the rate of methylene insertion is about two orders of magnitude faster than on Cu(110). As a result, two sequential methylene insertions are observed, and methyl groups are converted to propyl groups which undergo β-hydride elimination to evolve propylene. These results provide experimental precedence for the methylene insertion step in the carbide/methylene mechanism of Fischer–Tropsch catalysis and demonstrate the utility of copper as a catalyst for coupling hydrocarbon fragments.

2. EXPERIMENTAL

The experiments were performed in two ultra-high vacuum (UHV) systems. The Cu(110) studies were conducted in a UHV system equipped with capabilities for Auger electron spectroscopy (AES), low energy electron diffraction (LEED), temperature-programmed reaction (TPR) studies, ion sputtering, and H atom dosing (12). The Cu(100) experiments were carried out in an apparatus equipped with capabilities for AES, TPR, ion sputtering, H atom dosing, and high-resolution electron energy loss spectroscopy (HREELS) (13). The Cu(110) crystal used in these studies was a 0.7-cm diameter disk (Monocrystals Ltd., 99.999%) which was attached to a resistive heating element by three tantalum tabs bent over the edges of the crystal (12). The Cu(100) crystal (Monocrystals Ltd., 99.999%) was 1.0 cm in diameter and was tied to a resistive heating element by wrapping a chromel wire around the grooved edge of the crystal (13). Both samples could be heated to above 1000 K and cooled with liquid nitrogen to 110 K. The surface temperatures were measured with chromel alumel thermocouple junctions; for Cu(110) the junction was spot welded to one of the Ta tabs, while for Cu(100) the junction was wedged in a hole in the side of the crystal. The estimated absolute uncertainty in the temperature measurement during the TPR experiments is ±20 K, which reflects variable degrees of thermal contact between the thermocouple and the sample (12). The reproducibility for a given mounting scheme is closer to ±10 K. The surfaces were cleaned by Ar ion bombardment and annealing in vacuum as previously described (12, 13), and surface cleanliness before and after experiments was verified by AES.

In the TPR studies in both apparatus, the surface was exposed to gases by back-filling the chamber, and for coadsorption studies, the two reagents were dosed using separate leak valves to avoid cross contamination. The adsorbate-covered surface was then positioned 2 mm from a 2-mm diameter aperture into a shielded mass spectrometer pumped by either an ion or a turbo molecular pump. The surface was heated linearly at 2.5–4 K/s while up to three ion intensities were simultaneously monitored with a multiplexed Vacuum Generators SXP300 quadrupole mass spectrometer which (except for the experiments in Fig. 5) was operated at an electron impact ionization energy of 70 eV. Most of the alkyl halides used in these studies were obtained from Aldrich, stored in shielded glass vials, and used as received after several freeze–pump–thaw cycles with liquid nitrogen to remove volatile impurities. CD_2I_2 (98 at%) and C_2D_5I (99 at%) were obtained from Cambridge isotope Laboratories. Sample purities were verified *in situ* by mass spectrometry. Computer simulations of the TPR spectra were made by integrating the rate expressions using a variable-order, variable-time-step, backward differentiation formula integrator (14).

The HREELS spectrometer, which consists of single-pass 127° cylindrical monochromator and analyzer sectors (McAllister Technical), was operated at a beam energy of 3–5 eV and a resolution (FWHM) of 70–110 cm^{-1}. All spectra were taken in the specular direction ($\theta_{in} = \theta_{out} =$ 60° from the surface normal) at 110 K after briefly anneal-

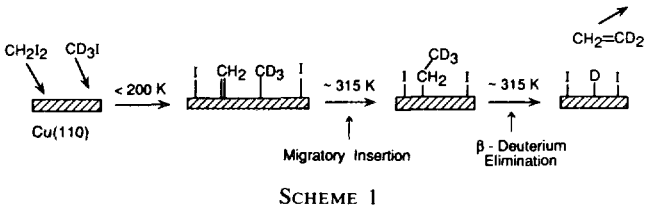

SCHEME 1

ing to the desired temperature. The change in the surface work function was measured by detecting the cutoff in the current to ground as a function of crystal bias when a low-energy (3–10 eV) electron beam from the Auger electron spectrometer was impinged onto the surface at normal incidence (15). All measurements were made with the sample at 120 K, and the electron currents in these studies were on the order of 10^{-8} A. Based on the energy spread in the incident electron beam, the experimental accuracy on a standard sample [CO/Cu(111)], and the experimental reproducibility (16), we estimate that the accuracy of the work function change measurements is ±50 meV.

3. RESULTS AND INTERPRETATION

The experimental results are reported below in five sections. The first three describe the formation and reactions of CH_3, C_2H_5, and CH_2 which are generated on Cu(100) by dissociative adsorption of CH_3I, C_2H_5I, and CH_2I_2, respectively. The results are similar to those published previously for these molecules on Cu(111) and Cu(110) surfaces, so the findings here on Cu(100) here are briefly summarized. The fourth section details the insertion reaction when methylene is coadsorbed with deuterated methyl and ethyl groups on the surface. Section five then compares the kinetics of this reaction on Cu(100) and Cu(110).

3.1. *Iodomethane (CH_3I)*

The reactions of iodomethane with a Cu(100) surface are similar in most respects to those previously reported for this molecule on Cu(110) (12) and Cu(111) (17). Carbon–iodine bond dissociation occurs at temperatures above 150 K (see the work function change measurements discussed in Section 3.3) to form adsorbed methyl groups and iodine atoms. The methyl groups are stable on the surface up to ~400 K, and above this temperature they react to evolve methane, ethylene, ethane, and propylene. The coverage dependence of these products is shown by the temperature-programmed reaction spectra in Fig. 2 for m/e = 16 (methane), m/e = 27 (ethylene and ethane), m/e = 30 (ethane), and m/e = 41 (propylene). Several aspects of the results deserve comment. First, all of the hydrocarbon products formed from CH_3I are evolved above 400 K, and their rate of evolution is determined by the rate of reaction as opposed to desorption (all of these hydrocarbons desorb below 250 K when adsorbed separately on Cu(100)). Second, since hydrogen atoms on copper (18) and iodine-covered copper (19) surfaces recombine and desorb between 300 and 400 K and no hydrogen desorption is detected, we can be sure that all C–H bonds remain intact in the methyl group up to 400 K. Third,

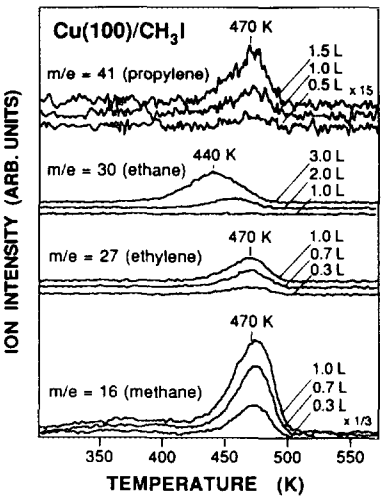

FIG. 2. Temperature-programmed reaction spectra of the methane, ethylene, ethane, and propylene produced after the indicated exposures of CH_3I on a Cu(100) surface at 300 K. The heating rates were 2.5 K/s.

Auger electron spectroscopy studies show no detectable carbon on the surface after heating to 600 K. Finally, recent studies of CH_3I on Cu(111) have shown that, in addition to the products mentioned above, methyl radicals are evolved from the surface at 475 K for CH_3I exposures above 1 L (20). The possibility of a similar reaction channel has yet to be investigated on Cu(100) and cannot be ruled out. Since the insertion reaction described below in Section 3.3 occurs below 300 K, such a high-temperature methyl radical ejection pathway is not an issue for the studies reported here.

An important conclusion from the TPR results in Fig. 2 is that, in the absence of coadsorbed species besides iodine atoms, methyl groups are thermally stable on Cu(100) up to 400 K. Figure 3 shows a vibrational spectrum of methyl groups formed on Cu(100) by annealing a 4.0-L exposure of CH_3I to 270 K to dissociate the C–I bond. This spectrum is similar to that for methyl groups formed on Cu(111) either by dissociation of CH_3I or by adsorption of methyl radicals (21). As discussed in Refs. (17) and (21), we assign this spectrum as follows: 370 cm^{-1} [ν(Cu–C)], 1150 cm^{-1} [$\delta_s(CH_3)$], 1430 cm^{-1} [$\delta_{as}(CH_3)$], 2760 and 2915 cm^{-1} [$\nu(CH_3)$]. The metal–methyl stretching frequency of 370 cm^{-1} is substantially lower than that of 450–650 cm^{-1} for methyl groups bound to a single metal atom in organometallic compounds (22), suggesting that the methyl groups bind in a higher coordination bridge or hollow site on the surface. The low frequency of 2760 cm^{-1} for some of the CH_3 stretching modes is characteristic of alkyl groups on copper surfaces, and appears to result from charge donation from the metal to the alkyl group (23).

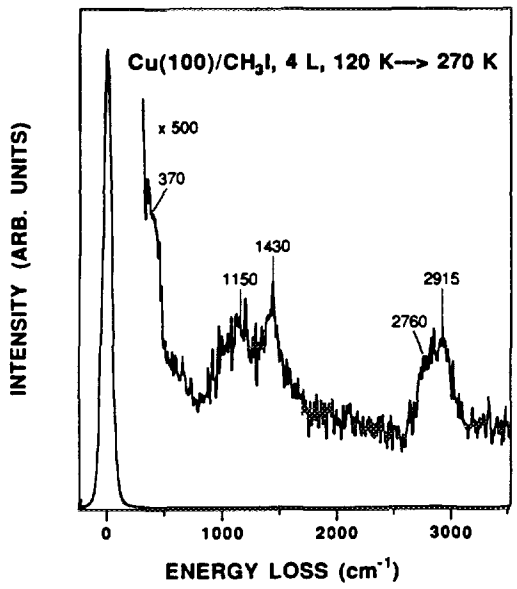

FIG. 3. Specular high-resolution electron energy loss spectrum of a monolayer of methyl groups and iodine atoms formed on Cu(100) by adsorbing 4 L of CH_3I at 120 K and annealling to 270 K to induce C–I bond dissociation.

3.2. *Iodoethane and Bromoethane (C_2H_5I and C_2H_5Br)*

Iodo- and bromoethane were used as precursors for forming ethyl groups on Cu(100). The reason for discussing the results for both compounds (the results are similar) is that HREELS spectra have been obtained only for C_2H_5Br, but C_2H_5I was used as the ethyl precursor in connection with the results in Section 3.4. When submonolayer coverages of these molecules are adsorbed on Cu(100), the C–I and C–Br bonds dissociate below 200 K to form adsorbed ethyl groups. Figure 4 shows a vibrational spectrum of these ethyl groups together with a temperature-programmed reaction spectrum of bromoethane reacting to form ethylene, which is the primary thermal decomposition product. The vibrational spectrum is similar to that reported for ethyl groups on Cu(111) (23). A key feature is the softened C–H stretching mode at 2730 cm^{-1} which is characteristic of the C–H bonds at the α-carbon in alkyl groups bonded to a copper surface (23). The evolution of ethylene at 245 K is the result of β-hydride elimination by the adsorbed ethyl groups. This reaction pathway has been previously established on a Cu(110) surface by isotope labeling studies (19); the peak temperature for the olefin product on Cu(100) as well as on Cu(111) (13) is 15–20 K high than on Cu(110). The hydrogen atoms that are transferred to the surface in the β-elmination reaction recombine and desorb as H_2 at 300–400 K or react with additional ethyl groups at 245 K to form ethane. The main point germane to the insertion experiments described below is that β-hydride elimination is a facile reaction which occurs at 230–250 K on Cu(100).

3.3. *Diiodomethane (CH_2I_2)*

When CH_2I_2 reacts with copper surfaces, the sole hydrocarbon product evolved is ethylene, and all CH_2 units are removed from the surface as judged by the absence of adsorbed carbon in AES studies and the reproducibility of multiple successive experiments in which the surface is annealed to 980 K to remove adsorbed iodine. Studies in which CH_2I_2 and CD_2I_2 are coadsorbed rule out reversible dehydrogenation of the methylene units. Selected temperature-programmed reaction spectra for the ethylene produced when 2 L of a CH_2I_2 (52%) and CD_2I_2 (48%) *mixture* is adsorbed onto Cu(100) at 110 K are shown in Fig. 5. The spectra of the indicated ions were obtained with an electron impact ionization energy of 20 eV to minimize cracking and accentuate the molecular ions. The absence of any detectable m/e = 31 beyond the 2% contribution of $C_2H_2D_2$ due to the 1% natural abundance of ^{13}C shows that CD_2CHD is not produced and that there is no isotope scrambling. Furthermore, as shown by the relative product yields in the inset, the $CH_2CH_2 : CH_2CD_2 : CD_2CD_2$ ratio of 1.0 : 1.8 : 1.0 indicates that the combination of the adsorbed methylene groups is nearly statistical. A similar result is also found for *sequential* adsorption of 0.5 L of CH_2I_2 and 0.5 L of CD_2I_2 as shown in Fig. 6. The relative product yields of CD_2CD_2 (monitored here by m/e = 30, $C_2D_3^+$), CD_2CH_2 (monitored by m/e = 29, CD_2CH^+), and CH_2CH_2 (monitored by m/e = 27, $C_2H_3^+$, which is also a cracking fragment of CH_2CD_2), after correcting for the cracking contributions and the ion detection sensitivities

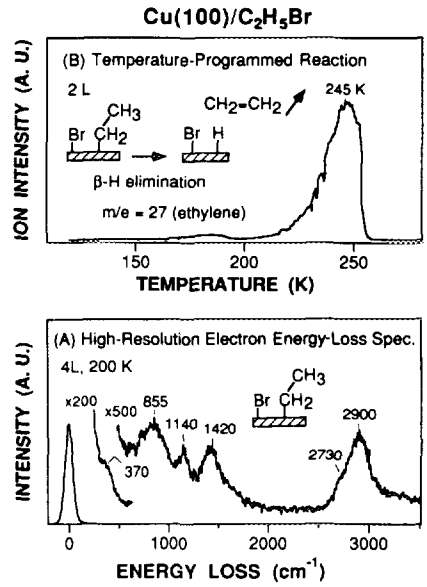

FIG. 4. (A) High-resolution electron loss spectrum (HREELS) and (B) temperature-programmed reaction (TPR) spectrum of $BrCH_2CH_3$ adsorbed on a Cu(100) surface. The inset schematics show the surface species and reactions to which the spectra are attributed. The heating rate in the TPR experiment was 2.5 K/s.

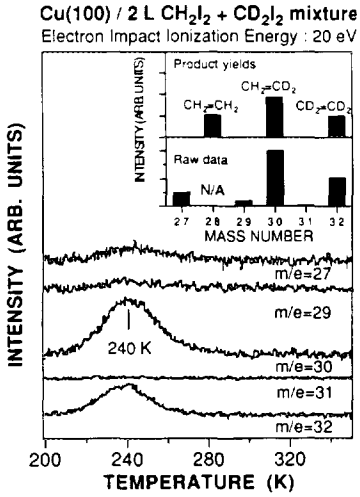

FIG. 5. Temperature-programmed reaction spectra for the indicated ions after exposing a Cu(100) surface at 110 K to 2 L of a CH_2I_2 (52%) and CD_2I_2 (48%) mixture. The surface heating rate was 3 K/s, and the electron impact ionization energy in the quadrupole mass spectrometer was 20 eV. The inset shows the relative ion intensities based on the TPR peak areas and the relative ethylene product yields after correcting for cracking patterns assuming that the isotopomers formed are CH_2CH_2, CH_2CD_2, and CD_2CD_2. The ion intensity at 28 amu (denoted as N/A in the inset) was not measured because of the large background in the mass spectrometer.

relative to the molecular ions, are shown in the top panel of Fig. 6. The 1.0 : 1.7 : 0.93 ratio observed for $C_2H_4 : C_2H_2D_2 : C_2D_4$ is approximately equal to that of 1 : 2 : 1 which would be expected for complete mixing and random combination of the CH_2 groups on the surface.

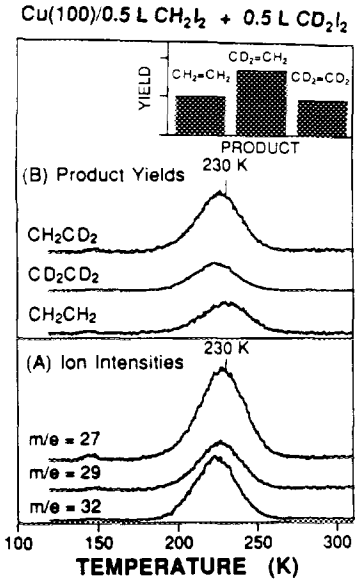

FIG. 6. (A) Ion intensities and (B) product yields for reaction of an equimolar mixture of CH_2I_2 and CD_2I_2 on Cu(100) to form various isotopes of ethylene. As discussed in the text, the product ratios provide evidence for random mixing and combination of the CH_2 units on the surface.

If the CH_2I_2 adsorbed first in this experiment were to form islands which did not mix with the subsequently adsorbed CD_2I_2 or if there were a significant deuterium isotope effect in the combination reaction, then a nonstatistical distribution would have been observed.

Ethylene evolution when CH_2I_2 is reacted with Cu(100) suggests formation and dimerization of CH_2. A number of observations indirectly support that CH_2I_2 dissociates on Cu(100) to form adsorbed CH_2 groups. Note in particular that ethylene is evolved from the surface at 250 K. This temperature is ~100 K above the temperature where ethylene desorbs from Cu(100). This observation indicates that the reaction that forms ethylene as opposed to ethylene desorption is the rate-determining step in ethylene evolution.

Dissociation of CH_2I_2 is also probably not the rate-determining step since the C–I bond in structurally similar CH_3I dissociates at ~170 K. Furthermore, based on the reactions of methyl and methylene halides with metal atoms in the gas phase (25), an even lower C–I bond dissociation temperature might be expected for CH_2I_2 compared with CH_3I. Dissociation of CH_2I_2 at comparable or lower temperatures than CH_3I is supported by the work function change measurements presented in Fig. 7. As shown in Fig. 7A, adsorption of 3L of CH_3I on Cu(100) lowers the surface work function by 0.75 eV. Such a decrease is typical of halogenated hydrocarbons on copper (13) and other metals (26). The increase in the surface work function between 140 and 200 K when the surface is heated is due to C–I bond dissociation as confirmed by HREELS studies (see above and Ref. (17)). CH_2I_2 on the other hand shows a different work function profile, as illustrated in Fig. 7B. Note in particular that the surface work function decreases very little when CH_2I_2 is adsorbed at 120 K, and that there is only a small change as a function of surface temperature. The dip between 120

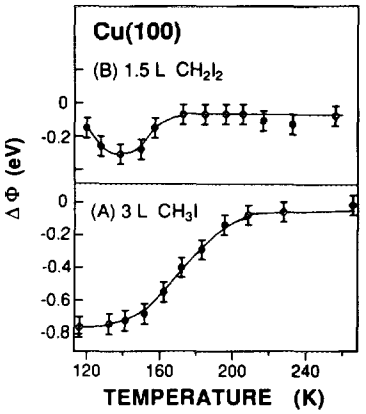

FIG. 7. Work function change as a function of surface temperature after the indicated exposures of (A) CH_3I and (B) CH_2I_2 to Cu(100). All measurements were made at 120 K after flashing the surface at 2.5 K/s to the desired temperature.

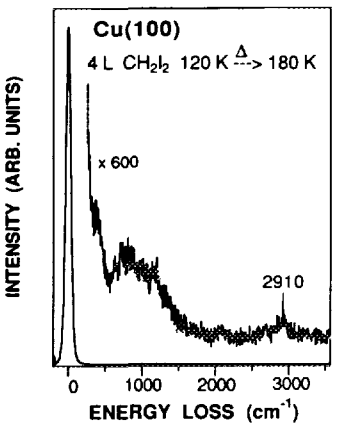

FIG. 8. Specular high-resolution electron energy loss spectrum of the monolayer formed by annealing a 4-L exposure of CH_2I_2 on Cu(100) to 180 K. As discussed in the text, chemical evidence suggests that this procedure dissociates the carbon–iodine bonds and produces a layer of CH_2 coadsorbed with iodine atoms.

and 160 K may indicate C–I bond scission, but it is also possible that C–I bond scission occurs upon adsorption at 120 K as it does for iodoethane (13), and that the small change reflects desorption of small amounts of coadsorbed water and/or CO (27). The possibility that only one C–I bond dissociates to form adsorbed CH_2I must also be considered. Ethylene could then be formed by CH_2I coupling to produce CH_2ICH_2I which dehalogenates. While the dehalogenation of 1,2-dihalocompounds is facile (28), the coupling of CH_2I species, if they were to form, appears unlikely at 250 K. For example, CH_3 coupling on Cu(100) does not occur until temperatures above 400 K (see Fig. 2).

HREELS spectra of the surface species formed when CH_2I_2 is adsorbed on Cu(100) and annealed to 180 K to insure dissociation are, unfortunately, not sufficient to definitively establish the presence of adsorbed CH_2. A sample spectrum of such a monolayer is shown in Fig. 8. There is evidence for CH_x stretching modes at 2910 cm^{-1}, but the losses in the fingerprint region are sufficiently weak and unresolved to preclude spectroscopic identification of the surface fragments. However, the chemical evidence presented above strongly suggests that CH_2I_2 dissociates on Cu(100) below 200 K to form adsorbed CH_2 groups.

One other aspect of CH_2I_2 adsorption on Cu(100) which should be mentioned is that at high coverages (exposures above ~2 L) a second, lower temperature ethylene desorption peak is observed in the TPR spectra. This peak, which occurs at the expected ethylene desorption temperature of ~180 K, may result from coupling of "free" methylene groups formed during C–I bond dissociation. In particular, recent studies of CH_2I_2 dissociation on aluminum surfaces have shown that CH_2 ejection into the gas phase occurs at 170 K and is accompanied by ethylene formation (29). A similar process may also occur on Cu(100), although we have yet to detect gas phase methylene as evidenced by careful studies of the m/e = 14 : 27 cracking pattern of the products. The important point for the methylene insertion results described below is that the studies here were carried out at low surface coverages and tests were performed to confirm that surface-bound methylene as opposed to "free" methylene is the reactive species. Note also that evolution of ethylene at 180 K for high surface coverages of CH_2I_2 indicates that, at least under these conditions, both C–I bonds are cleaved by 180 K.

3.4. *Methylene Insertion (CH_2I_2 + CD_3I)*

Temperature-programmed reaction spectra of selected ions after coadsorbing 0.5 L of CH_2I_2 with 2 L of CD_3I on Cu(100) are shown in Fig. 9. Based on the results in the previous sections, the following peaks are expected if there is no reaction between CH_2I_2 and CD_3I: one peak for m/e = 27 at ~230 K for ethylene evolution from the reaction of CH_2I_2 and one each for m/e = 20 and 30 at ~470 K for methane and ethylene/ethane formation from CD_3I. However, in addition to these peaks, low temperature peaks are observed for m/e = 20 at 315 K and for m/e = 30 at 270 K, as well as a higher temperature shoulder for m/e = 27 at 270 K. These new features indicate a reaction between CH_2I_2 and CD_3I. The mass spectromet-

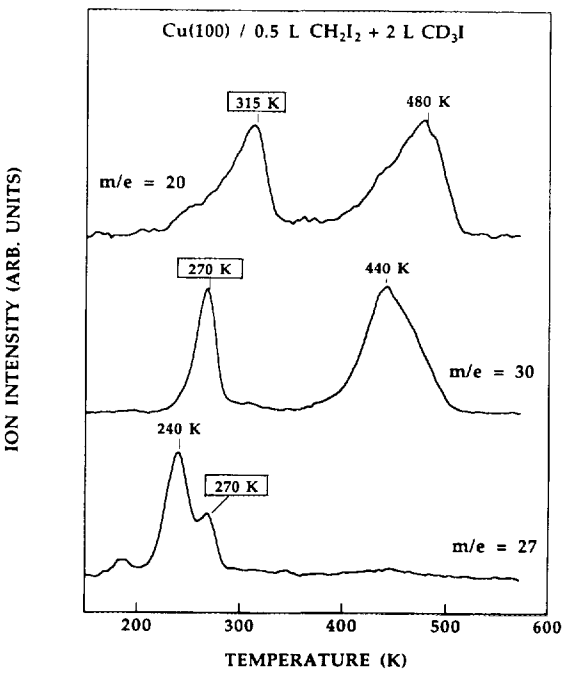

FIG. 9. Temperature-programmed reaction spectra of the indicated ions after adsorbing 0.5 L of CH_2I_2 followed by 2.0 L of CD_3I on Cu(100) at 120 K. The heating rates were 2.5 K/s. The temperatures in boxes indicate peaks that are not observed when the two constituents are adsorbed separately on the surface.

ric identification of these cross reaction products has been discussed previously in detail for the analogous reaction on Cu(110) (11), and it was shown that the new peak at 270 K is due to evolution of ethylene-d_2, while the peak at 315 K is due to CD_4. Also, from mass balance, the isotope composition of the products, and the reaction kinetics, it was established that methylene insertion/β-elimination was responsible for these products as shown in Scheme 2.

Similar conclusions are also valid here on Cu(100). A significant difference, however, is that while only a single methylene insertion was observed on Cu(110), two sequential CH_2 insertions are possible on Cu(100) as shown by the TPR results in Fig. 10. Figure 10A shows TPR spectra for m/e = 44, 45, and 46 after coadsorbing 0.5 L of CH_2I_2 with 2.0 L of CD_3I. The evolution of these ions at 240 K indicates that a 3-carbon product(s) containing deuterium is (are) formed. The 1.00 : 0.97 : 0.03 ratio of the peak areas is consistent with the literature cracking ratio (24) of 0.96 : 1.00 : 0.03 for propylene-3,3,3-d_3 (m/e = 45); the presence of m/e = 46 is due to the 1.1% natural abundance of ^{13}C. The formation of propylene-d_3, together with the absence of lower and higher isotopes of propylene, supports the reaction scheme shown in the inset where two CH_2 sequentially insert followed by β-hydride elimination. The dependence of the propylene-d_3 product yield on the coadsorbed CD_3I exposure is shown by the m/e= 45 TPR spectra in the top panel of Figure 10B. The nonlinear dependence of the yield on CD_3I exposure will be discussed further in Section 4.2. There is no evidence for C_4 products as evidenced by studies monitoring masses between 56 and 60.

To test the potential roles of surface segregation and/or radical and carbene formation during carbon–iodine bond dissociation, the order of halide precursor adsorption and dissociation was varied. Selected results are shown by the TPR spectra of the propylene-d_3 product (m/e = 45) in Fig. 11. In Figs. 11A and 11B, the order of CH_2I_2 and CD_3I adsorption was interchanged, while in Figs. 11C and 11D the CH_2I_2 and CD_3I monolayers were preannealed to dissociate the C–I bonds prior to adsorbing the other constituent. In all cases, the spectra are virtually identical in peak temperature, shape, and area. These results indicate that the adsorption sequence does not affect the surface reaction pathway, kinetics, or yield, and that radical or carbene formation during C–I bond dissociation is not an issue in these studies.

Methylene insertion into ethyl groups on Cu(100) is illustrated by the studies with C_2H_5I and C_2D_5I in Fig. 12.

$CH_2 + CD_3 \longrightarrow CH_2CD_3$ Migratory Insertion
$CH_2CD_3 \longrightarrow CH_2CD_2 + D$ β - Elimination
$D + CD_3 \longrightarrow CD_4$ Reductive Elimination

SCHEME 2

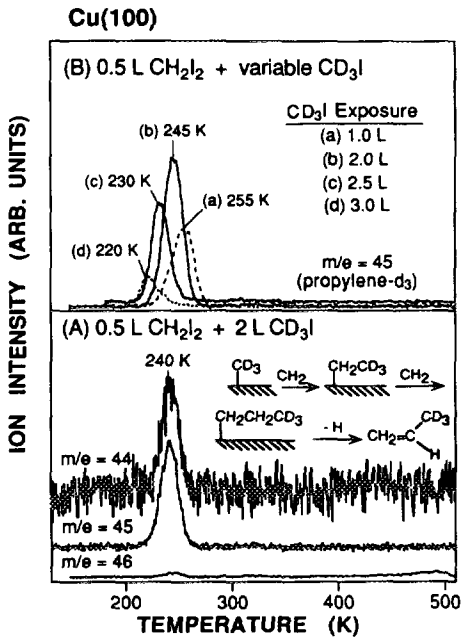

FIG. 10. Temperature-programmed reaction spectra of the propylene-d_3 formed when CH_2I_2 and CD_3I are reacted on a Cu(100) surface. (A) Diagnostic ion intensities for the propylene-3,3,3-d_3 product formed by methylene insertion/β-elimination as indicated in the inset schematic. (B) Dependence of the propylene-d_3 TPR spectra on CD_3I exposure. The heating rates were 2.5 K/s.

Here, reaction of CH_2I_2 with C_2H_5I produces propylene (m/e = 42), while reaction with C_2D_5I produces propylene-d_4 (m/e = 46). These are the expected products of CH_2 insertion into the metal–carbon bond to form propyl groups followed by β-elimination of a hydrogen or deuterium atom as shown by the inset schematics. The 20-K higher peak temperature for evolution of propylene-d_4 relative to propylene as well as the dramatically different

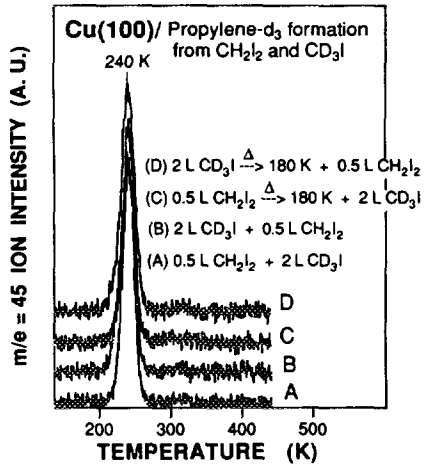

FIG. 11. Effect of dosing order and preannealing to dissociate C–I bonds on the kinetics and yield of propylene-d_3 (m/e = 45) formed by reacting 0.5-L CH_2I_2 with 2-L CD_3I on a Cu(100) surface.

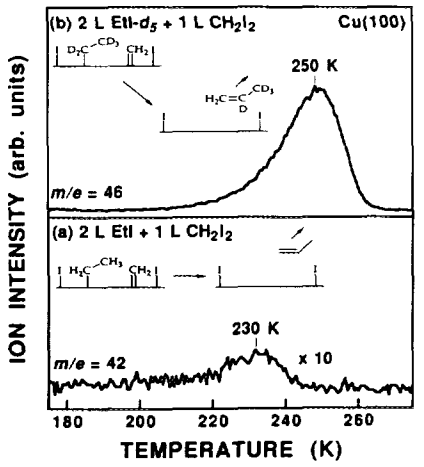

FIG. 12. Temperature-programmed reaction spectra for (a) propylene (m/e = 42) and (b) propylene-d_4 (m/e = 46) formed by reacting C_2H_5I and C_2D_5I, respectively, with CH_2I_2 on Cu(100). The surface heating rates were 4 K/s.

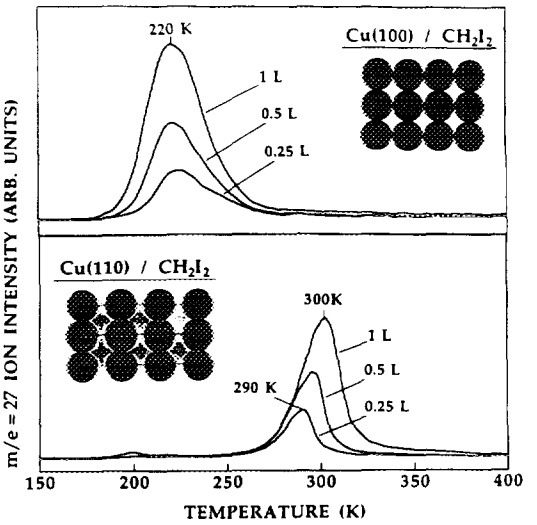

FIG. 13. Comparison of the TPR spectra for the ethylene formed by reaction of CH_2I_2 on Cu(100) and Cu(110). Top views of the atom configurations on these surfaces are shown in the insets. The heating rates in these experiments were 2.5 K/s.

yields for the two products indicates a deuterium isotope effect which will be discussed further in Section 4.2. The possibility of C_4 products from these reactions was not, unfortunately, investigated, but butene formation would be expected for the $CH_2 + C_2D_5$ system analogous to propylene formation from $CH_2 + CD_3$. C_4 products are unlikely for the $CH_2 + C_2H_5$ reaction because of the substantially faster rate of β-elimination for hydrogen vs deuterium (note the small yield of propylene relative propylene-d_4 in Fig. 12).

3.5. *Cu(100) versus Cu(110)*

As mentioned above, a major difference between the methylene insertion reaction on Cu(100) and Cu(110) is formation of C_3 products on Cu(100) and their absence on Cu(110). The origin of this difference lies in the relative rates of chain propagation, chain termination, and reactant consumption by side reactions on these surfaces. The three competing processes for methylene insertion on copper surfaces are shown in Scheme 3.

Chain growth occurs by methylene insertion, chain termination by β-hydride elimination, and CH_2 coupling is a side reaction that depletes the supply of surface methylene. The rate of methyl decomposition is orders of magnitude slower than these reactions on both surfaces and need not be considered here.

In comparing the rates of the reactions above on Cu(100) and Cu(110), we find that β-hydride elimination

Chain Propagation:	$CH_2 + CH_3$	$\longrightarrow CH_2CH_3$
Chain Termination:	CH_2CH_3	$\longrightarrow CH_2CH_2 + H$
Side Reaction:	$CH_2 + CH_2$	$\longrightarrow CH_2CH_2$

SCHEME 3

occurs with a TPR peak temperature of 250 ± 10 K on Cu(100) and 230 ± 10 K on Cu(110). Methylene coupling, on the other hand, is substantially slower on Cu(110) than on Cu(100) as shown by the TPR results in Fig. 13. CH_2I_2 produces ethylene at ~300 K on Cu(110) vs ~220 K on Cu(100). Note also the different coverage dependences and peak shapes on these two surfaces. Furthermore, neither surface shows the peak temperature shift to lower values with increasing coverage as is expected for a rate-determining bimolecular process (30). These points will be discussed further in Section 4.2.

Like CH_2 coupling, the rate of methylene insertion on Cu(110) is dramatically slower than the rate on Cu(100). This difference is illustrated by the TPR spectra in Fig. 14. Here it is seen that the insertion reaction (as measured by evolution of ethylene-d_2 (m/e = 30) when CH_2I_2 and CD_3I are coadsorbed) occurs with about a 50-K higher peak temperature on Cu(110) than on Cu(100). (The small yield of ethylene-d_2 at 245 K on Cu(110) and the difference between the coverage dependences of the reaction kinetics on Cu(100) and Cu(110) will be discussed in Section 4.2.) The point we emphasize here is that a 50-K temperature difference in a TPR experiment corresponds to about two orders of magnitude in rate at 300 K (31).

As mentioned, the fact that propylene is formed on Cu(100) and not Cu(110) reflects the relative rates of the three reactions described above: CH_2 coupling, CH_2 insertion, and β-elimination. Neglecting for the moment the possibility of multiple insertions, the yield of ethylene from the first insertion step is determined by the relative rates of CH_2 insertion and coupling. Since both reactions are slower by a comparable amount on Cu(110) vs

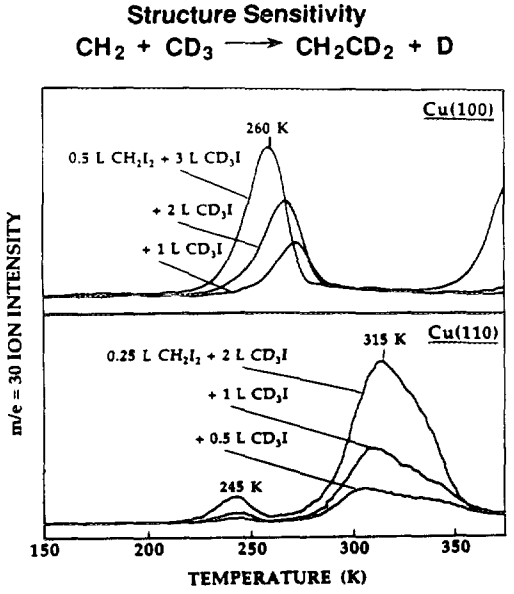

FIG. 14. Comparison of the TPR spectra for formation of ethylene-d_2 (m/e = 30) when the indicated exposures of CH_2I_2 and CD_3I are reacted on Cu(100) and Cu(110) surfaces. The substantial difference between the peak temperatures (260 vs 315 K) on these surfaces indicates that the reaction rate is dependent on the structure of the metal surface. The small peak at 245 K in the (110) spectra may indicate reaction at "(100)-type" defect sites on this surface; the leading edge above 350 K in the (100) spectra is a cracking fragment of ethane-d_6 formed by coupling of adsorbed CD_3 groups (compare Fig. 2). The surface heating rates in these experiments were 2.5 K/s.

Cu(100), the yield of ethylene is relatively insensitive to surface geometry (see Fig. 14). The yield of propylene from the second insertion step, however, also depends on the relative rate of β-elimination which converts ethyl groups to ethylene. Thus, while chain growth by methylene insertion and chain termination by β-hydride elimination occur at similar rates on Cu(100) (TPR peak temperatures = 250–270 K), the insertion reaction is about two orders of magnitude slower than β-hydride elimination on Cu(110). The slower rate of chain propagation relative to termination is the primary reason for the lack of propylene formation on Cu(110). These factors are discussed more fully below.

4. DISCUSSION

4.1. Insertion Mechanism

The temperature-programmed reaction results presented above show that reaction of CH_2I_2 and CD_3I on a Cu(100) surface leads to carbon–carbon bond formation and evolution of ethylene-d_2 and propylene-d_3. Here, we discuss two key aspects of the mechanism: (1) that C–C bond formation involves adsorbed CH_2 and CD_3 as opposed to species containing carbon–iodine bonds or free radical intermediates formed during C–I bond dissociation, and (2) that the mechanism of C–C bond formation involves migratory insertion of CH_2 into the metal–carbon bond of adsorbed CD_3.

The evidence that C–C bond formation involves adsorbed CH_2 and CD_3 is both direct and indirect. In the case of CD_3I, the TPR, HREELS, and work function change measurements all establish that C–I bond dissociation occurs below 180 K to produce adsorbed methyl groups. Therefore, since preannealing a submonolayer coverage of CD_3I to 180 K has no noticeable effect on the propylene formation rate or yield in the coadsorption experiments with CH_2I_2 (see Fig. 11D), we can conclude that adsorbed CD_3 and not CD_3I or a CD_3 radical formed during C–I bond dissociation is the active species in C–C bond formation. For CH_2I_2, there is indirect evidence that annealing to 180 K induces C–I bond dissociation and formation of adsorbed CH_2. Specifically, the work function change measurements in Fig. 7B suggest that C–I bond dissociation may occur even at the adsorption temperature of 120 K. Scission of *both* C–I bonds at this temperature is also suggested by the evolution of ethylene at 230 K when submonolayer coverages of CH_2I_2 are heated; one would not expect a CH_2I species to couple at such a low temperature given that CH_3 coupling occurs above 400 K. Provided C–I bond scission does occur below 180 K to form adsorbed CH_2, as these results suggest, the preannealing experiment in Fig. 11C establishes that adsorbed CH_2 and not CH_2I_2 or CH_2I is the active intermediate in C–C bond formation. The strongest evidence, however, that iodine-containing species are not involved in C–C bond formation is that propylene is also formed at 470 K during decomposition or methyl monolayers on Cu(100) (see Fig. 2). In this case, there is conclusive evidence (see above) that no C–I bonds remain intact. It is likely that propylene is formed as a result of methyl decomposition to methylene followed by sequential methylene insertion into unreacted methyl groups as discussed previously in connection with the chemistry of methyl groups on Cu(110) (12).

Related to the issue of adsorbed fragments containing C–I bonds is the effect of coadsorbed iodine atoms on the reactions of adsorbed methyl and methylene. In the case of methyl groups, the iodine effect has been addressed on Cu(111) by forming methyl groups on the surface in either the presence or absence of iodine atoms using a methyl radical source (21). The main effect of the coadsorbed iodine atoms is to block surface sites. For low coverages of iodine there is no significant effect on the methyl decomposition products or kinetics. At higher coverages, there is a crossover from methyl decomposition to methyl radical desorption, and it appears that this effect is due to blocking of surface defects by the coadsorbed iodine atoms (21). Similar studies have

yet to be performed for adsorbed CH_2, but based on the TPR results in Fig. 13, the effect of coadsorbed iodine atoms is not substantial; i.e., there is no dramatic shift of the TPR peak temperature with increasing surface coverage.

We now consider the evidence that CH_2 insertion is the mechanism for forming ethylene-d_2 and propylene-d_3 from the reaction of CH_2 and CD_3 on Cu(100). As mentioned in Section 3, the isotope distribution in the products strongly supports the methylene insertion/β-elimination mechanism. The ethylene product contains two deuteriums (see Ref. (11) for a detailed discussion of the mass spectrometric identification), the propylene product contains three deuteriums, and when ethyl-d_5 groups are reacted with CH_2, the product propylene contains four deuterium atoms. Each is consistent with CH_2 insertion followed by β-elimination. Also, the evolution of methane-d_4 at 315 K when CH_2 and CD_3 are reacted provides additional evidence for the β-elimination reaction. Specifically, the deuterium atoms produced on the surface by β-elimination combine with remaining CD_3 on the surface to produce CD_4. Not only is the CD_4 peak temperature consistent with that for reaction of methyl groups and adsorbed D atoms (12), but, as discussed previously for Cu(110) (12), the product ratio of methane-d_4 at 315 K to ethylene-d_2 is $\sim$1 as expected from mass balance (32).

The isotope distribution of the products also rules out other possible mechanisms for C–C bond formation. For example, if more highly dehydrogenated intermediates are involved, isotope scrambling would be expected. We can also rule out the possibility that propylene is formed by reaction of ethylene with adsorbed methyl groups (a Ziegler–Natta-type olefin insertion reaction). In this case, one would expect not only propylene-d_3 from insertion of C_2H_4 (the CH_2 coupling product) into CD_3 but also propylene-d_4 and propylene-d_5 from insertion of ethylene-d_2 into adsorbed methyl groups. The absence of m/e = 46 intensity beyond that expected for the ^{13}C contribution to propylene-d_3 in the TPR results of Fig. 10A rules out this possibility.

4.2. *Insertion Kinetics*

Three aspects of the insertion reaction kinetics will be discussed: isotope effects, coverage dependences, and the effect of surface geometry. Because CH_2 coupling and β-hydride elimination occur concurrently and in competition with CH_2 insertion, a change in the relative rates of these processes also changes the branching ratio between the various pathways. The combined effect of changes in relative rates and yields produces TPR signatures that are not readily deciphered. This point is illustrated by the deuterium isotope effect for the reaction of CH_2I_2 with C_2H_5I and C_2D_5I to form propylene (Fig. 12). While propylene-d_4 is evolved with a 20-K higher TPR peak temperature than propylene consistent with the 10–20 K deuterium isotope effect for β-elimination (19), the dramatic difference in yields (note that the m/e = 42 peak in Fig. 12A has been multiplied by a factor of 10) indicates that β-hydride elimination cannot be the sole rate-determining step in both cases. In particular, if CH_2 insertion were rapid compared with β-elimination, then (barring a substantial isotope effect for insertion) both C_2H_5I and C_2D_5I should produce comparable amounts of propylene. Instead, in the C_2D_5I reaction, insertion competes favorably with β-elimination which is slowed by the deuterium isotope effect, but for C_2H_5I, β-elimination predominates over insertion, and almost no propylene is formed. The combination of these two effects prohibits a more quantitative analysis of the isotope effect.

The effects of competing surface reactions are also apparent in the coverage dependence of the propylene-d_3 yield from the reaction of CH_2I_2 and CD_3I. As shown in Fig. 10B, increasing the exposure of CD_3I first increases and then decreases the yield of propylene-d_3. This behavior reflects two competing effects of increasing the CD_3 concentration. One is to increase the rate of formation of the initial insertion product CH_2CD_3 which in turn increases the rate of propylene formation. The other is to decrease the available surface coverage of CH_2 which decreases the rate of propylene formation. The net effect can be shown quantitatively by computer simulation of the TPR spectra as illustrated in Fig. 10 and discussed below.

In simulating the TPR spectra for the reaction of CH_2 with CD_3 on Cu(100) there are nine reactions which have been experimentally demonstrated and which must be considered. These reactions, which are largely the same as those considered previously for Cu(110) (12), are listed in Table 1. Independent determinations of the pre-expo-

TABLE 1

Reactions and Activation Energies[a] Used to Simulate the Temperature-Programmed Reaction Spectra of CH_2 + CD_3 on Cu(100)

Reaction	Activation energy (kcal/mol)
$CD_3 \rightarrow CD_2 + D$	31
$D + CD_2 \rightarrow CD_3$	18
$CH_2 + CD_3 \rightarrow CH_2CD_3$	14
$CH_2CD_3 \rightarrow CH_2CD_2 + D$	17
$CH_2 + CH_2CD_3 \rightarrow CH_2CH_2CD_3$	14
$CH_2CH_2CD_3 \rightarrow CH_2CHCD_3 + H$	15
$D + CD_3 \rightarrow CD_4$	16.5
$D + D \rightarrow D_2$	20
$CH_2 + CH_2 \rightarrow CH_2CH_2$	13

[a] Pseudo first order preexponential factors of 10^{13} s^{-1} were used in each case.

nential factors and activation energies for these nine reactions are not possible given the current data. In the case of Cu(110), however, sufficient experiments were performed to determine the *rate constants* with reasonable accuracy. Specifically, pseudo first order pre-exponential factors of 10^{13} s^{-1} were assumed for each reaction and the activation energies were calculated to reproduce the TPR peak temperatures and yields. Note that, even though the pre-exponential factors will in reality differ from 10^{13} s^{-1}, the choice of the activation energy to reproduce the TPR peak temperature compensates for errors in the prefactor. In other words, inaccuracies in the preexponential factor and activation energy for a given reaction compensate one another so that the magnitude of the *rate constant* will be quite accurate over a limited temperature range (a factor of 3 in the rate constant shifts the TPR peak by ~10 K for reactions occurring at 200–300 K).

The way in which peak temperatures and product yields are used to determine the reaction activation energies has been discussed previously for Cu(110) (12). Since many of the results on Cu(100) are the same to within the ±20 K uncertainty in the TPR peak temperatures, the same parameters have been applied with several exceptions. Most notably the activation energies for CH_2 insertion and coupling have been lowered by 5 kcal/mol to reproduce the lower peak temperatures on Cu(100).

The resulting simulation of the TPR products for the reaction of $5 \times 10^{+12}$ CH_2/cm^2 and $1.5 \times 10^{+13}$ CD_3/cm^2 (coverages comparable to those present in the experiments (12)) is shown in Fig. 15A. The products formed in order of increasing temperature are ethylene from CH_2 coupling (240 K), propylene-d_3 from two sequential CH_2 insertions followed by β-elimination (255 K), ethylene-d_2 from CH_2 + CD_3 followed by β-elimination (275 K), CD_4 from D + CD_3 (305 K), and C_2D_4/CD_4 from CD_3 disproportionation (470 K). Not only are the product peak temperatures comparable to those measured experimentally, but the relative product yields are also similar—stringent criteria for the rate constants. The effect of varying the CD_3 coverage on the propylene-d_3 peak temperature and yield is shown in Fig. 15B. The maximum in the product yield and the decrease in the peak temperature with increasing CD_3 coverage are consistent with the experimental results in Fig. 10B. These results indicate that activation energies in Table 1 in conjunction with pseudo first order preexponential factors of 10^{13} s^{-1} provide reasonable rate constants for the indicated surface reactions on Cu(100).

We now turn to the substantial difference between the rates of methylene coupling and insertion on Cu(100) and Cu(110). As noted previously, the 50–80-K lower TPR peak temperatures for insertion and coupling on Cu(100) correspond to about two orders of magnitude larger in rate (31). Several observations suggest that the slower rates on Cu(110) are due to rate-determining diffusion of

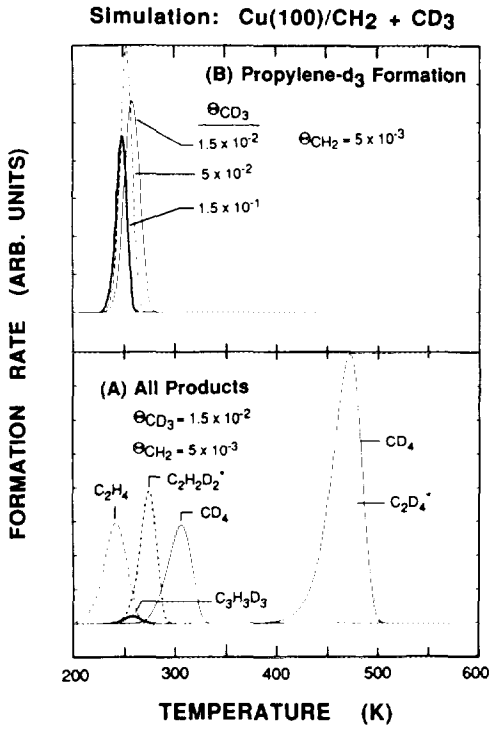

FIG. 15. Simulated TPR spectra of (A) the products from reaction of CH_2 and CD_3 and (B) the dependence of the propylene-d_3 product yield on CD_3 exposure. Coverages are reported as number of adsorbates per surface copper atom. The ethylene formed by methylene insertion/β-elimination is denoted with an asterisk to distinguish it from ethylene formed by methylene coupling. The kinetic parameters used in these simulations are described in the text and summarized in Table 1. The parameters were chosen to qualitatively reproduce the experimental results in Figs. 9 and 10.

CH_2 on this surface. Note, for example, that both coupling and insertion occur at ~300–320 K on Cu(110) (see Figs. 13 and 14). Note also that there is a lower temperature peak in each case that also increases with exposure and which occurs at approximately the same temperature as that for the corresponding reaction on Cu(100). We suggest that these peaks indicate some "(100)-type" (33) sites on the Cu(110) surface. In any event, it is clear that some of the CH_2 groups react at a significantly lower temperature than the majority of surface species and if CH_2 diffusion were rapid, it is difficult to envision why all of the adsorbed CH_2 would not react at these lower temperatures.

Rate-determining diffusion, however, cannot account for the non-second order behavior of the TPR peak temperature with exposure (see Section 3.5). To account for both the rate and coverage dependence of the CH_2 coupling and insertion reactions on Cu(110) we propose that the reaction occurs by rate-determining diffusion of CH_2 to "(100)-type" defect sites on the surface. Evidence for such sites where the reaction is fast and for rate-determining CH_2 diffusion has been presented above. We show

here how such a model can give rise to pseudo first order reaction kinetics for methylene insertion. The reactive "(100)-type" sites are denoted with an asterisk, and, for purposes of illustration, we assume that CD_3 diffusion is rapid both to and from the reactive sites. The critical component in the kinetic model for achieving pseudo first order kinetics is that once CH_2 groups reach the reactive sites they react before diffusing away again; rapid diffusion of CD_3 insures that methyl groups are always present at the active site so that (provided reaction with CH_2 is rapid compared with CH_2 diffusion) diffusion of CH_2 to the active sites can be written as an irreversible step. Furthermore, if we approximate the rate of diffusion to active sites as a bimolecular reaction between the active site and the diffusing species (34), the resulting kinetic system is shown in Scheme 4. Applying the steady state approximation to the reactive species gives

$$\frac{dC_2H_4^*}{dt} = k_1\theta_{CH_2}\theta_*.$$

As evidenced by this relation, rate-determining diffusion of CH_2 to selected active sites on the surface can produce a kinetic rate law that is not first order in both CH_2 and CH_3 coverage. It should be emphasized, however, that other scenarios are also possible and that the actual situation is more complex than that described above. For example, the presence of coadsorbed iodine atoms has been neglected. The purpose of this discussion was to illustrate how the combination of slow CH_2 diffusion and the presence of selected active sites on Cu(110), two features for which there is some experimental evidence, could give rise to the observed kinetics. Additional experiments (for example, variation of the CH_2 coverage for a fixed CD_3 coverage) are needed to substantiate this kinetic model.

4.3. Comparison with Other Metals

In comparing the chemistry of methyl and methylene on copper surfaces under vacuum conditions with that on other transition metal surfaces, copper is the only one to date that has been reported to catalyze alkyl chain propagation by methylene insertion. In most other cases, however, coadsorption of methylene with methyl has not been studied. One might expect that in the case of methyl adsorption alone, methylene insertion would be observed since dehydrogenation of methyl groups produces methylene on the surface. In actuality, only hydrogenation and dehydrogenation have been reported in the reaction of methyl groups on Ni (35), W (36), Fe (37), Pd (38), Co (39), and Pt (40) surfaces. Silver does form C–C bonds, but via coupling of alkyl groups (26, 41).

$$CH_2 + * \xrightarrow{k_1} CH_2^*$$
$$CH_3 + * \underset{k_{-2}}{\overset{k_2}{\rightleftharpoons}} CH_3^*$$
$$CH_2^* + CH_3^* \xrightarrow{k_3} C_2H_5^*$$
$$C_2H_5^* \xrightarrow{k_4} C_2H_4^* + H^*$$

SCHEME 4

No doubt one of the reasons copper catalyzes methylene insertion is that it is relatively inert towards dehydrogenation of methyl and methylene, whereas dehydrogenation reactions occur preferentially on most other metals. While the facility of the insertion reaction on copper may seem surprising, recent calculations have predicted that this pathway should have a lower activation energy on Cu than on Pt, Ni, and Fe (42). It should also be noted that the low temperature coupling observed for CH_2 on Cu(110) is consistent with the formation of ethylene in the classic studies of Brady and Pettit, in which diazomethane (a CH_2 source) was reacted with copper catalysts (8b).

Finally, it is worth noting that copper's reputation as a relatively inert catalyst stems from its inability to dissociatively adsorb most stable molecules. This inactivity in turn reflects the thermodynamic fact that copper makes relatively weak bonds to adsorbates. What the studies here and calculations elsewhere (42) show is that if hydrocarbon fragments can be generated on a copper surface, then a remarkable number of bond-breaking and bond-forming transformations are possible under quite mild conditions. These transformations can take place because the hydrocarbon fragments are bound strongly enough to the surface that molecular desorption of the fragments does not compete kinetically with reaction on the surface. The somewhat unexpected facility of the transformations on the surface (many of the reactions occur below 300 K) arises, thermodynamically, from the fact that *both* the reactants and products are relatively weakly bound to the surface compared with other transition metals. As a result, ΔH for many of these reactions on copper is comparable to that for the analogous process on more "active" metals such as platinum (12, 42). This finding may shed some light on the utility of copper in bimetallic catalysts. Conversely, one might view these findings as a cautionary note for those attempting to elucidate the role of "inert" constituents in bimetallic catalysts. That neither constituent in a bimetallic catalyst shows the activity of the combined catalyst does not necessarily imply the importance of bimetallic sites. Synergistic effects of the two *pure* metals must also be considered. The more active metal may generate surface fragments which the less active metal can then selectively manipulate to form the desired product. In this respect, a bimetallic catalyst would perform as a true bifunctional catalyst where the active metal initiates the reaction and the inactive metal completes the catalysis. Further study is needed to investigate this possibility in bimetallic catalysts.

5. CONCLUSIONS

The results above show that when CH_2I_2 and CD_3I are reacted on a Cu(100) surface, carbon–carbon bond formation occurs to produce ethylene-d_2 and propylene-d_3. Both products are evolved from the surface at 250–270 K, and mechanistic studies suggest the following sequence of events: C–I bond dissociation below 200 K to form adsorbed CH_2 and CD_3 groups, followed by methylene insertion at 250–270 K to form adsorbed CH_2CD_3 and $CH_2CH_2CD_3$ which undergo β-hydride elimination to produce the partially deuterated olefins. HREELS, work function change measurements, and TPR studies provide direct evidence for formation of adsorbed CD_3 and indirect evidence for formation of adsorbed CH_2. The existence and kinetics of the β-hydride elimination pathway have been independently confirmed using iodo- and bromoethane as precursors to form adsorbed ethyl groups. The relative rates of methylene insertion and β-hydride elimination on Cu(100) limit the maximum chain length of the hydrocarbon product to three carbons as confirmed by computer simulation of the TPR experiments using the measured kinetic parameters. Comparison of these results with previous results for Cu(110) shows that the insertion reaction is structure sensitive, being a factor of ~100 faster on Cu(100) than on Cu(110). Based on the kinetics for methylene coupling and insertion on these two surfaces, it is suggested that the substantially slower rates on Cu(110) are due to slow diffusion of CH_2 to defect sites, which are the reactive sites, on this surface.

ACKNOWLEDGMENTS

Financial support from the National Science Foundation (Grant CHE-90-22077) and from the Joint Services Electronics Program through the Columbia Radiation Laboratory (Contract DAAL03-91-C-0016) is gratefully acknowledged. Acknowledgment is also made to the Donors of the Petroleum Research Fund, administered by the American Chemical Society, for the partial support of this research. C.-M. C. gratefully acknowledges a predoctoral fellowship from IBM.

REFERENCES

1. Fischer, F., and Tropsch, H., *Chem. Ber.* **59,** 830 (1926).
2. For reviews of the Fischer–Tropsch reaction see, for example, (a) Anderson, R. B., "The Fischer–Tropsch Synthesis." Academic Press, New York, 1984; (b) Rofer-DePoorter, C. K., *Chem. Rev.* **81,** 447 (1981); (c) Herrmann, W. A., *Angew. Chem., Int. Ed. Engl.* **21,** 117 (1982); (d) Biloen, P., and Sachtler, W. M. H., *Adv. Catal.* **30,** 165 (1981).
3. For examples of the importance of the concentration and 2-dimensional configuration of adsorbed species in initiating bimolecular synthesis reactions, see (a) Gurney, B. A., and Ho, W., *J. Chem. Phys.* **87,** 1376 (1987); (b) Yang, Q. Y., Johnson, A. D., Maynard, K. J., and Ceyer, S. T., *J. Am. Chem. Soc.* **111,** 8748 (1989).
4. For a clear and concise summary of evidence for the carbide/methylene mechanism, see Zheng, C., Apeloig, Y., and Hoffmann, R., *J. Am. Chem. Soc.* **110,** 749 (1988).
5. Bonzel, H. P., and Krebs, H. J., *Surf. Sci.* **91,** 499 (1980).
6. (a) Biloen, P., Helle, J. N., and Sachtler, W. M. H., *J. Catal.* **58,** 95 (1979); (b) Biloen, P., *Recl. Trav. Chim. Pays-Bas* **99,** 33 (1980); (c) Goodman, D. W., *Acc. Chem. Res.* **17,** 194 (1984); (d) Geerlings, J. J. C., Zonnevylle, M. C., and de Groot, C. P. M., *Surf. Sci.* **241,** 302 (1991).
7. (a) Baker, J. A., and Bell, A. T., *J. Catal.* **78,** 165 (1982); (b) Wang, C. J., and Ekerdt, J. G., *J. Catal.* **86,** 239 (1984).
8. (a) Blyholder, G., and Emmett, P. H., *J. Phys. Chem.* **63,** 962 (1959); *J. Phys. Chem.* **64,** 470 (1959); (b) Brady, R. C. III, and Pettit, R., *J. Am. Chem. Soc.* **102,** 6182 (1980); *J. Am. Chem. Soc.* (1981); (c) Brock, H., Tschmutowa, G., and Wolf, H. P., *J. Chem. Soc., Chem. Commun.*, 1068 (1986).
9. See, for example, (a) McBreen, P. H., Erley, W., and Ibach, H., *Surf. Sci.* **148,** 292 (1984); (b) Radloff, P. L., Mitchell, G. E., Greenlief, C. M., White, J. M., and Mims, C. A., *Surf. Sci.* **183,** 377 (1987); (c) Henderson, M. A., Radloff, P. L., White, J. M., and Mims, C. A., *J. Phys. Chem.* **92,** 4111 (1988); (d) Monim, S. S., and McBreen, P. H., *Surf. Sci.* **264,** 341 (1992).
10. (a) Zaera, F., *Acc. Chem. Res.* **25,** 260 (1992) and references therein; (b) Zhou, X.-L., Zhu, X.-Y., and White, J. M., *Surf. Sci. Rep.* **13,** 74 (1991) and references therein.
11. Chiang, C.-M., Wentzlaff, T. H., Jenks, C. J., and Bent, B. E., *J. Vac. Sci. Technol., A* **10,** 2185 (1992).
12. Chiang, C. M., Wentzlaff, T. H., and Bent, B. E., *J. Phys. Chem.* **96,** 1836 (1992).
13. Lin, J.-L., and Bent, B. E., *J. Phys. Chem.* **96,** 8529 (1992).
14. Shampine, L. F., and Watts, H. A., "DEPAC—Design of a User Oriented Package of ODE Solvers." SAND79-2374, Sandia Laboratories, 1979.
15. Mate, C. M., Kao, C.-T., and Somorjai, G. A., *Surf. Sci.* **206,** 145 (1988).
16. Xi, M., and Bent, B. E., *Surf. Sci.* **278,** 19 (1992).
17. Lin, J.-L., and Bent, B. E., *J. Vac. Sci. Technol., A* **10,** 2202 (1992).
18. Anger, G., Winkler, A., and Rendulic, K. D., *Surf. Sci.* **220,** 1 (1989).
19. Jenks, C. J., Bent, B. E., Bernstein, N., and Zaera, F., *J. Am. Chem. Soc.* **115,** 308 (1993).
20. Lin, J.-L., and Bent, B. E., *J. Phys. Chem.* **97,** 9713 (1993).
21. Chiang, C.-M., and Bent, B. E., *Surf. Sci.* **279,** 79 (1992).
22. Maslowsky, E., Jr., "Vibrational Spectra of Organometallic Compounds." Wiley, New York, 1977.
23. Lin, J.-L., and Bent, B. E., *Chem. Phys. Lett.* **194,** 208 (1992).
24. Stenhegen, E., Abrahamsson, S., and McLafferty, F. W. (Eds.), "Atlas of Mass Spectral Data." Interscience, New York (1969).
25. Polanyi, J. C., *Chem. Phys. Lett.* **1,** 421 (1967).
26. (a) Zhou, X.-L., Solymosi, F., Blass, P. M., Cannon, K. C., and White, J. M., *Surf. Sci.* **219,** 294 (1989); (b) Zhou, X. L., and White, J. M., *Catal. Lett.* **2,** 375 (1989).
27. CO and H_2O desorb from Cu(100) between 100 and 200 K: Lin, J.-L., and Bent, B. E., unpublished results.
28. Walter, W. K. and Jones, R. G., *Surf. Sci.* **2674,** 391 (1992); Kadodwala, M., and Jones, R. G., *J. Vac. Sci. Technol., A* **11,** 2019 (1993); Bent, B. E., Nuzzo, R. G., Zegarski, B. R., and Dubois, L. H., *J. Am. Chem. Soc.* **113,** 1143, 1991.
29. Domen, K., and Chuang, T. J., *J. Am. Chem. Soc.* **109,** 5288 (1987).
30. Redhead, P. A., *Vacuum* **12,** 203 (1962).
31. Typically, reaction rates increase by an order of magnitude for every 20–30 K increase in temperature. For example, a first order reaction whose TPR peak is at 250 K will have an activation energy of ~15 kcal/mol for a typical pre-exponential factor of 10^{13} s^{-1}. Increasing the temperature to 270 K increases the rate by an order of magnitude.

Conversely, reactions which occur around room temperature and whose TPR peaks differ by 20–30 K will have rates that differ by about an order of magnitude if the rates could be measured for both reactions at the same temperature.

32. The ratio of methane-d_4 to ethylene-d_2 is slightly less than one because some surface D atoms are scavenged by CH_2 groups to make CH_2D [12].
33. The reactive sites need not necessarily be of (100) geometry. Other crystal planes such as (111) may also have reaction rates comparable to that on (100).
34. In treating the kinetics of adsorbate diffusion to defect sites on the surface as a bimolecular reaction (i.e., first order in the concentration of both adsorbates and defects) we are assuming that the adsorbates and defects are randomly distributed across the surface.

35. (a) Zhou, X.-L., and White, J. M., *Surf. Sci.* **194,** 438 (1988); (b) Marsh, E. P., Tabares, F. L., Schneider, M. R., Gilton, T. L., Meier, W., and Cowin, J. P., *J. Chem. Phys.* **92,** 2004 (1990).
36. Zhou, X.-L., Yoon, C., and White, J. M., *Surf. Sci.* **206,** 379 (1980).
37. Benziger, J. B., and Madix, R. J., *J. Catal.* **65,** 49 (1980).
38. Solymosi, F., and Revesz, K., *J. Am. Chem. Soc.* **113,** 9145 (1991).
39. Steinbach, R., Kiss, J., Krall, R., *Surf. Sci.* **157,** 401 (1985).
40. (a) Henderson, M. A., Mitchell, G. E., and White, J. M., *Surf. Sci.* **184,** L325 (1987); (b) Zaera, F., *Surf. Sci.* **219,** 453 (1989); (c) Radhakrishnan, G., Stanzel, W., Hemmen, R., Conrad, H., and Bradshaw, A. M., *J. Chem. Phys.* **95,** 3930 (1991).
41. Zhou, X. L., and White, J. M., *J. Phys. Chem.* **95,** 5575 (1991).
42. (a) Shustorovich, E., *Catal. Lett.* **7,** 107 (1990); (b) Shustorovich, E., and Bell, A. T., *Surf. Sci.* **248,** 359, 1991.